Available online at www.sciencedirect.com
SCIENCE DIRECT
Journal of Sound and Vibration 294 (2006) 410–417
JOURNAL OF SOUND AND VIBRATION
www.elsevier.com/locate/jsvi

Short Communication

A steady-state equilibrium configuration in the dynamic analysis of a curved pipe conveying fluid

Duhan Jung[a], Jintai Chung[b,*]

[a]*Department of Precision Mechanical Engineering, Graduate School, Hanyang University, 17 Haengdang-dong, Seongdong-gu, Seoul 133-791, Republic of Korea*
[b]*Department of Mechanical Engineering, Hanyang University, 1271 Sa-1-dong, Ansan, Kyunggi-do 425-791, Republic of Korea*

Received 11 July 2005; received in revised form 4 November 2005; accepted 19 November 2005
Available online 24 January 2006

Abstract

This paper discusses a steady-state equilibrium configuration and a set of linearized equations of motion for the dynamic analysis of a semi-circular fluid-conveying pipe. Through application of the perturbation method to the equations of motion for a semi-circular pipe, new nonlinear equilibrium equations were derived and the equations of motion were linearized around the equilibrium configuration of the pipe. The equilibrium configurations obtained from the derived nonlinear equilibrium equations were compared to configurations from the linear equilibrium equations of other researchers. Additionally, the natural frequencies computed in this study were compared with the frequencies presented in a previous study. It was found that the steady-state equilibrium configuration should be determined using the proposed nonlinear equilibrium equations rather than previous linear equilibrium equations. Furthermore, it was shown that the natural frequencies computed with the proposed equilibrium equations were more accurate than the frequencies of other studies.

1. Introduction

The dynamic characteristics of pipes conveying fluid have been investigated by many researchers because of their technological importance. Many papers have considered straight pipes to analyse pipe vibrations and stability; curved pipes, on the other hand, have attracted relatively little attention. Since most piping systems are composed of both straight and curved pipes, considerable research concerning the dynamics of curved pipes is required to reduce the vibrations of systems and guarantee their stability.

An early analytical model for the dynamics and stability of a curved pipe conveying fluid was suggested by Chen [1,2], who assumed that the centreline of the curved pipe is inextensible. Chen claimed that the curved pipe shows instability similarly to a straight pipe when the fluid velocity exceeds a certain critical value. Hill and Davis [3], as well as Doll and Mote [4], found that if the centreline is extensible, a fluid-conveying curved pipe does not lose stability, even for high fluid velocities. On the other hand, Misra et al. [5,6] analysed and

*Corresponding author. Tel.: +82 31 400 5287; fax: +82 31 406 5550.
E-mail address: jchung@hanyang.ac.kr (J. Chung).

0022-460X/$ - see front matter © 2006 Elsevier Ltd. All rights reserved.
doi:10.1016/j.jsv.2005.11.016

compared the dynamics for two cases of fluid-conveying curved pipes with extensible and inextensible centrelines. They concluded that the dynamic analysis of curved pipes with an extensible centreline is more reasonable than analysis with an inextensible centreline.

However, the study on the extensible curved pipe by Misra et al. [6] was based on the assumption of small pipe deformation, which is valid only when the fluid velocity is relatively low. Under this assumption, the steady-state equilibrium equations of the curved pipe become linear and the equations of motion linearized around an equilibrium configuration are identical to the equations presented by Misra et al. [6]. When the pipe deformation is not small, the natural frequencies computed with these equilibrium and linearized equations can differ largely from the actual natural frequencies. Thus, it is also valuable to investigate the equilibrium configuration and the natural frequencies of a pipe with large deformation.

This study discusses equations for steady-state equilibrium and equations of motion linearized around an equilibrium configuration for a semi-circular fluid-conveying pipe. After applying the perturbation method to the nonlinear equations of motion for the semi-circular pipe, nonlinear steady-state equilibrium equations and equations of motion linearized in the neighbourhood of an equilibrium configuration were derived. The derived equilibrium equations are different from the corresponding equations presented in Ref. [6]; that is, the former is nonlinear and the latter is linear. Steady-state equilibrium configurations computed with both the linear and nonlinear equilibrium equations were compared and verified. Furthermore, after establishing three types of modelling for the equilibrium equations and the linearized equations, the natural frequencies computed through use of these models were evaluated and compared.

2. Equations of motion

A semi-circular pipe conveying fluid, shown in Fig. 1, was considered for investigation of the steady-state equilibrium configuration and linearized equations of motion. A curved pipe with a centreline radius R is clamped at both the ends and conveys fluid with a constant velocity U. The cross-sectional area, the area moment of inertia about the z-axis, and Young's modulus of the pipe are denoted by A, I and E, respectively. The pipe mass and fluid mass per unit length are given by m_p and m_f, respectively. This paper assumes that the pipe is slender and extensible, that the flow is an inviscid plug flow, and that the effect of gravity is negligible.

The equations of motion used in this study are equivalent to the equations presented by Misra et al. [6], where only the in-plane motion of the semi-circular pipe conveying fluid is considered. This study uses an xyz coordinate system fixed to the pipe to express the equations of motion for the semi-circular pipe. The x and y axes are in the radial and circumferential directions of the pipe centreline, respectively, and the z-axis is perpendicular to the plane containing the pipe centreline. The angle θ is measured from the X-axis fixed in space. The radial and circumferential displacements of a point on the pipe centreline are denoted by u and v, respectively. Using the notation given above, the nonlinear equations of in-plane motion presented in Ref. [6] can be rewritten as

$$(m_p + m_f)\ddot{u} + 2m_f(U/R)(\dot{u}' - \dot{v}) + m_f(U/R)^2(u'' - v') + EI(u^{\mathrm{iv}} - v''')/R^4 + EA(u + v')/R^2 - EA[(u + v')(u' - v)]'/R^3 = m_f U^2/R, \quad (1)$$

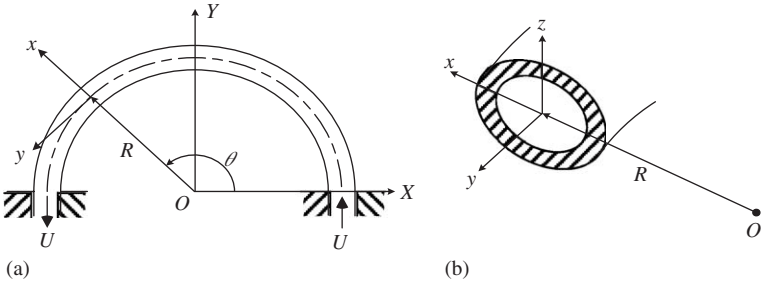

Fig. 1. Semi-circular pipe conveying fluid with velocity U: (a) top view and (b) cross-section.

$$(m_p + m_f)\ddot{v} + m_f(U/R)(\dot{u} + \dot{v}') + m_f(U/R)^2(u' - v) + EI(u''' - v'')/R^4 - EA(u' + v''')/R^2 - EA(u + v')(u' - v)/R^3 = 0, \tag{2}$$

where the superposed dot represents the derivative with respect to time, and the prime represents the derivative with respect to θ. The clamped–clamped boundary conditions of the pipe are given by

$$u = u' = v = 0 \quad \text{at } \theta = 0, \pi. \tag{3}$$

The steady-state equilibrium configuration and the equations linearized in the neighbourhood of the equilibrium configuration were obtained by applying the perturbation method to Eqs. (1) and (2). In accordance with the perturbation method, displacements can be expressed as the sum of the steady-state equilibrium displacement and the perturbed displacement around the equilibrium displacements. The radial displacement u and the circumferential displacement v may be represented by

$$u = u_e + \Delta u, \quad v = v_e + \Delta v, \tag{4}$$

where u_e and v_e are the displacements corresponding to the equilibrium configuration and Δu and Δv are the perturbed displacements of u and v around the equilibrium configuration. Because u_e and v_e have constant values in a steady state, their derivatives with respect to time become zero. Therefore, when Eqs. (4) are substituted into Eqs. (1) and (2), the steady-state equilibrium equations and the linearized equations of motion can be derived. The derived equilibrium equations are

$$m_f(U/R)^2(u_e'' - v_e') + EI(u_e^{\mathrm{iv}} - v_e''')/R^4 + EA(u_e + v_e')/R^2 - EA[(u_e + v_e')(u_e' - v_e)]'/R^3 = m_f U^2/R, \tag{5}$$

$$m_f(U/R)^2(u_e' - v_e) + EI(u_e''' - v_e'')/R^4 - EA(u_e' + v_e'')/R^2 - EA(u_e + v_e')(u_e' - v_e)/R^3 = 0. \tag{6}$$

The equations of motion linearized in the neighbourhood of the equilibrium configuration are given by

$$(m_p + m_f)\ddot{u} + 2m_f(U/R)(\dot{u}' - \dot{v}) + m_f(U/R)^2(u'' - v') + EI(u^{\mathrm{iv}} - v''')/R^4 + EA(u + v')/R^2 - EA[(u_e + v_e')(u' - v)]'/R^3 - EA[(u_e' - v_e)(u + v')]'/R^3 = 0, \tag{7}$$

$$(m_p + m_f)\ddot{v} + m_f(U/R)(\dot{u} + \dot{v}') + m_f(U/R)^2(u' - v) + EI(u''' - v'')/R^4 - EA(u' + v'')/R^2 - EA(u_e + v_e')(u' - v)/R^3 - EA(u_e' - v_e)(u + v')/R^3 = 0, \tag{8}$$

where Δ is deleted from Δu and Δv for simplicity of notation. Note that Eqs. (5) and (6) are nonlinear ordinary differential equations. Eqs. (7) and (8) become linear partial differential equations after u_e and v_e are determined; also, it should be noted that Eqs. (7) and (8) are influenced by the equilibrium configuration, because they include u_e and v_e.

3. Discretization

Approximate solutions were obtained for the equilibrium equations and the linearized equations of motion through the use of the Galerkin method. In order to find approximate solutions in finite-dimensional function spaces, both the equilibrium equations and the linearized equations of motion were discretized with the assumption that the solutions are linear combinations of the basis functions. The radial and circumferential displacements representing the equilibrium configuration can be expressed as

$$u_e(\theta) = \sum_{n=1}^{N} X_n^e U_n(\theta), \quad v_e(\theta) = \sum_{n=1}^{N} Y_n^e V_n(\theta), \tag{9}$$

where N is the total number of basis functions; X_n^e and Y_n^e are constants to be determined; and $U_n(\theta)$ and $V_n(\theta)$ are the basis functions selected as comparison functions:

$$U_n(\theta) = \cosh \lambda_n\theta - \cos \lambda_n\theta - \frac{\cosh \pi\lambda_n - \cos \pi\lambda_n}{\sinh \pi\lambda_n - \sin \pi\lambda_n}(\sinh \lambda_n\theta - \sin \lambda_n\theta), \tag{10}$$

$$V_n(\theta) = \sin n\theta, \tag{11}$$

where λ_n are the roots of

$$\cosh \pi\lambda_n \cos \pi\lambda_n - 1 = 0. \tag{12}$$

Eqs. (10) and (11) are well-known eigenfunctions for the bending and axial vibrations of a beam, respectively. Similarly, the radial and circumferential displacements for the perturbed motion may be represented by

$$u(t,\theta) = \sum_{n=1}^{N} X_n(t) U_n(\theta), \quad v(t,\theta) = \sum_{n=1}^{N} Y_n(t) V_n(\theta), \tag{13}$$

where $X_n(t)$ and $Y_n(t)$ are functions of time.

The discretized equations are obtained by application of the Galerkin method to Eqs. (5)–(8) with the series solutions of Eqs. (9) and (13). These discretized equations can be represented by vector equations; the equilibrium equations may be expressed as

$$(\mathbf{K} + U^2\mathbf{H})\mathbf{X}^e + \mathbf{N}(\mathbf{X}^e) = U^2\mathbf{F}, \tag{14}$$

where $\mathbf{K}$ is the structural stiffness matrix, $\mathbf{H}$ is the matrix related to the centrifugal fluid force, $\mathbf{N}(\mathbf{X}^e)$ is the nonlinear force vector, $\mathbf{F}$ is the external force vector due to the fluid flow, and $\mathbf{X}^e$ is an unknown vector given by

$$\mathbf{X}^e = \{X_1^e, Y_1^e, X_2^e, Y_2^e, \ldots, X_N^e, Y_N^e\}^{\mathrm{T}}. \tag{15}$$

The equations of motion linearized around the equilibrium configuration can be represented by

$$\mathbf{M}\ddot{\mathbf{X}}(t) + 2U\mathbf{G}\dot{\mathbf{X}}(t) + (\mathbf{K} + \mathbf{K}_T + U^2\mathbf{H})\mathbf{X}(t) = \mathbf{0}, \tag{16}$$

where $\mathbf{M}$ is the mass matrix, $\mathbf{G}$ is the matrix related to the gyroscopic force, $\mathbf{K}_T$ is the tangential stiffness matrix, and $\mathbf{X}(t)$ is an unknown vector given by

$$\mathbf{X}(t) = \{X_1(t), Y_1(t), X_2(t), Y_2(t), \ldots, X_N(t), Y_N(t)\}^{\mathrm{T}}. \tag{17}$$

Note that the size of all the matrices is $2N \times 2N$ and the size of all the vectors is $2N \times 1$.

4. Discussion

The following material properties and dimensions were used in this study: $m_p = m_f = 1.78\,\mathrm{kg/m}$, $E = 10\,\mathrm{GPa}$, $R = 0.5\,\mathrm{m}$, $A = 2.473 \times 10^{-4}\,\mathrm{m}^2$ and $I = 7.491 \times 10^{-8}\,\mathrm{m}^4$. For convenience of comparison between computed results, the dimensionless natural frequency $\overline{\omega}$ and the dimensionless fluid velocity $\overline{U}$ were introduced as follows:

$$\overline{\omega}_n = \omega_n R^2 \sqrt{\frac{m_p + m_f}{EI}}, \quad \overline{U} = UR\sqrt{\frac{m_f}{EI}}, \tag{18}$$

where ω_n is the natural frequency of the fluid-conveying pipe.

To verify the computation results presented in this paper, the convergence characteristics of the natural frequencies were investigated with the discretized equations. For this study, when the number of basis functions increased, the convergences of the natural frequencies were examined for the following two cases: zero fluid velocity and non-zero fluid velocity. The convergence characteristics of the three lowest natural frequencies when the fluid is stationary are shown in Table 1. This table shows that the natural frequencies converge as N increases. The converged values are close to the natural frequencies of the semi-circular beam presented by Blevins [7]. As shown in Table 2, even when the fluid velocity is not zero or when $\overline{U} = 2$, the natural frequencies still converge with increasing N. The convergence tests show that ten basis functions are sufficient to obtain accurate solutions. For this reason, all further computations in this study were performed with $N = 10$.

The differences between this study and Ref. [6] can be clarified by a comparison between the equilibrium equations and the linearized equations of motion given by Eqs. (5)–(8), and the corresponding equations presented in Ref. [6]. Using the notation of this paper, the equilibrium equations of Ref. [6] can be expressed as

Table 1
Convergence characteristics of the three lowest dimensionless natural frequencies when $\overline{U} = 0$

N	$\overline{\omega}_1$	$\overline{\omega}_2$	$\overline{\omega}_3$
1	31.847	31.913	—
2	16.813	25.370	42.236
3	4.552	19.169	33.079
4	4.449	9.663	27.721
5	4.383	9.624	17.861
6	4.379	9.494	17.837
7	4.371	9.493	17.690
8	4.371	9.476	17.690
9	4.369	9.476	17.668
10	4.369	9.472	17.668
Ref. [7]	4.385	9.633	17.620

Table 2
Convergence characteristics of the three lowest dimensionless natural frequencies when $\overline{U} = 2$

N	$\overline{\omega}_1$	$\overline{\omega}_2$	$\overline{\omega}_3$
1	30.555	33.364	—
2	16.788	25.453	42.311
3	4.424	19.290	33.159
4	4.031	10.096	27.635
5	3.998	9.520	18.248
6	3.968	9.468	17.322
7	3.963	9.430	17.284
8	3.960	9.421	17.221
9	3.960	9.416	17.213
10	3.959	9.414	17.203

$$m_f(U/R)^2(u_e'' - v_e') + EI(u_e^{\mathrm{iv}} - v_e''')/R^4 + EA(u_e + v_e')/R^2 = m_f U^2/R, \tag{19}$$

$$m_f(U/R)^2(u_e' - v_e) + EI(u_e''' - v_e'')/R^4 - EA(u_e' + v_e'')/R^2 = 0. \tag{20}$$

These are the linearized versions of Eqs. (5) and (6). By contrast, the linearized equations of motion given in Ref. [6] do not have the last terms on the left-hand sides of Eqs. (7) and (8); therefore, they can be rewritten as

$$\begin{aligned}(m_p + m_f)\ddot{u} + 2m_f(U/R)(\dot{u}' - \dot{v}) + m_f(U/R)^2(u'' - v') + EI(u^{\mathrm{iv}} - v''')/R^4 \\ + EA(u + v')/R^2 - EA[(u_e + v_e')(u' - v)]'/R^3 = 0,\end{aligned} \tag{21}$$

$$\begin{aligned}(m_p + m_f)\ddot{v} + m_f(U/R)(\dot{u} + \dot{v}') + m_f(U/R)^2(u' - v) + EI(u''' - v'')/R^4 \\ - EA(u' + v'')/R^2 - EA(u_e + v_e')(u' - v)/R^3 = 0.\end{aligned} \tag{22}$$

The deformed shape of the pipe was computed with both the linear and nonlinear equilibrium equations when the semi-circular fluid-conveying pipe is in steady-state equilibrium. The equilibrium configurations are presented in Fig. 2, where the deformed shapes are magnified by a factor of 5. Figs. 2a–c correspond to the deformed configurations in steady-state equilibrium when $\overline{U} = 2, 3$, and 4, respectively. In these figures, the dash–dotted lines represent the initial configuration of the pipe, or the steady-state configuration when $\overline{U} = 0$. The deformed configurations shown by the solid line were obtained by solving the nonlinear equilibrium equations of Eqs. (5) and (6). Additionally, the configurations of the dashed lines are obtained by solving the linear equilibrium equations of Eqs. (9) and (10). As shown in Fig. 2, the difference between the deformed

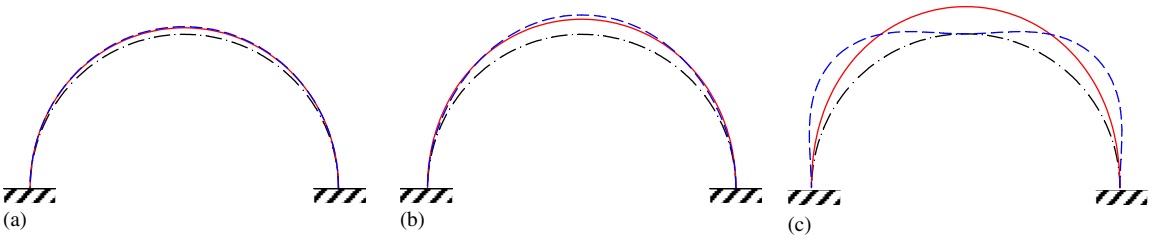

Fig. 2. Steady-state equilibrium configurations of the semi-circular pipe conveying fluid when: (a) $\overline{U} = 2$; (b) $\overline{U} = 3$; and (c) $\overline{U} = 4$. Initial configuration (dash–dotted line); configuration for the nonlinear equilibrium equations (solid line); and configuration for the linearized equations (dashed line).

Table 3
Three models of the steady-state equilibrium equations and the linearized equations of motion for the semi-circular pipe conveying fluid

Case	Steady-state equilibrium equations	Linearized equations of motion
Model I (proposed)	Nonlinear equations of Eqs. (5) and (6)	Eqs. (7) and (8)
Model II	Linear equations of Eqs. (19) and (20)	Eqs. (7) and (8)
Model III (Ref. [6])	Linear equations of Eqs. (19) and (20)	Eqs. (21) and (22)

shapes for the linear and nonlinear equilibrium equations is small when the fluid velocity is relatively low; however, the difference becomes large with high fluid velocity. Furthermore, in Fig. 2c, the deformed shape obtained from the linear equation exhibits fluctuation in the radial displacement, which cannot be explained from a physical point of view. Therefore, it is reasonable to say that the linearized equilibrium equations cannot be applied to the steady-state equilibrium configuration with large deformations. In other words, when the fluid velocity is high, the nonlinear equilibrium equations should be used instead of the linearized equations.

Next, some modelling issues regarding the steady-state equilibrium equations and the linearized equations of motion for the semi-circular pipe conveying fluid will be discussed. For convenience, three types of models are introduced when computing the natural frequencies of the semi-circular pipe. A model proposed in this paper, Model I, adopts Eqs. (5) and (6) as the nonlinear equilibrium equations and Eqs. (7) and (8) as the equations of motion linearized around the equilibrium configuration. Model II uses the same equations of motion as Model I, but selects the linear equations (19) and (20) as the equilibrium equations instead of the nonlinear equations. Finally, Model III, which is equivalent to the model presented in Ref. [6], consists of the steady-state equilibrium equations of Eqs. (19) and (20) and the linearized equations of motion, Eqs. (21) and (22). These three models are listed in Table 3.

The natural frequencies of the fluid-conveying semi-circular pipe were investigated for all models mentioned above. The three lowest dimensionless natural frequencies of the semi-circular pipe are presented for variations of the dimensionless fluid velocity in Fig. 3. Figs. 3a–c depict the natural frequencies for the first, second and third modes, respectively. In these figures, the natural frequencies for Models I, II and III are represented by solid, dashed, and dotted lines, respectively. As illustrated in Fig. 3, the differences in natural frequencies between Models I and III increased with fluid velocity. However, the natural frequencies of Model II demonstrated different behaviours for the variation of the fluid velocity as compared to the other models, particularly for the range $\overline{U} = 3$–4. In this range, the curve of the natural frequencies for Model II appears to have discontinuities. In fact, a sudden change of the equilibrium configurations was observed when they were computed with the linear equilibrium equations, Eqs. (19) and (20). This sudden change is shown in Fig. 4, in which the deformations are described on a true scale. As shown in Fig. 4, the equilibrium configurations obtained from the linear equations exhibit a large difference, even though the fluid velocity is changed only slightly (from $\overline{U} = 3.7$ to 3.8). In contrast, there is only a small difference in the configurations from the nonlinear equations of Eqs. (5) and (6). Therefore, it may be concluded that the equilibrium configuration obtained from the nonlinear equations is more reasonable than the configuration from the linear equations. The three lowest dimensionless

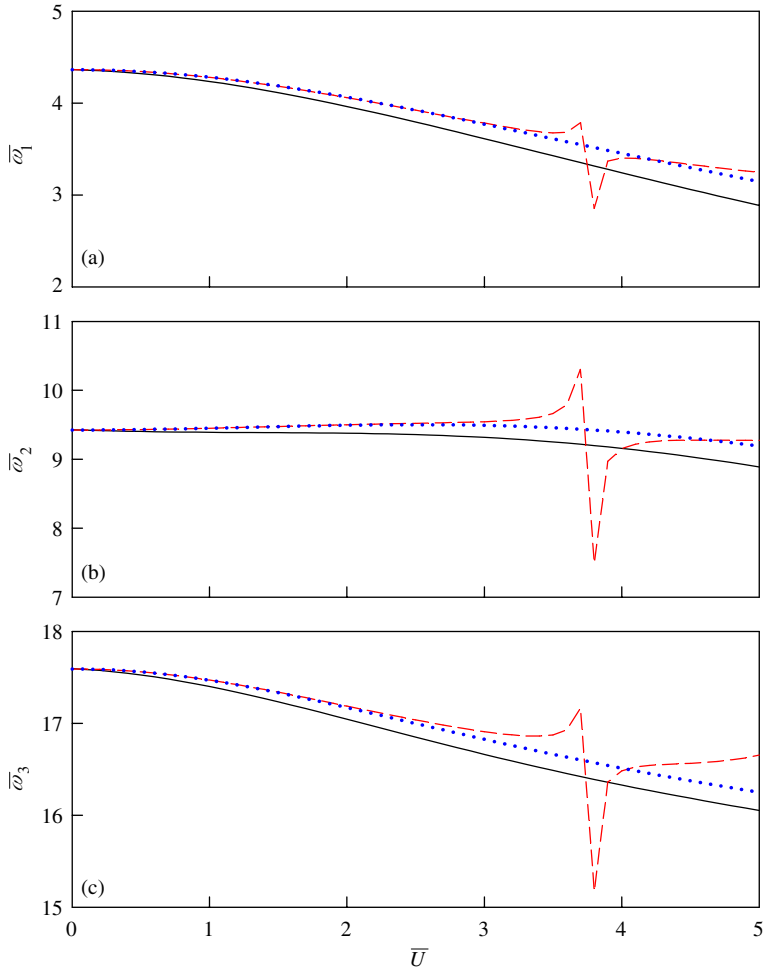

Fig. 3. The three lowest dimensionless natural frequencies of a semi-circular pipe conveying fluid with variation of the dimensionless fluid velocity: (a) first mode; (b) second mode; and (c) third mode. Model I (solid line); Model II (dashed line); and Model III (dotted line).

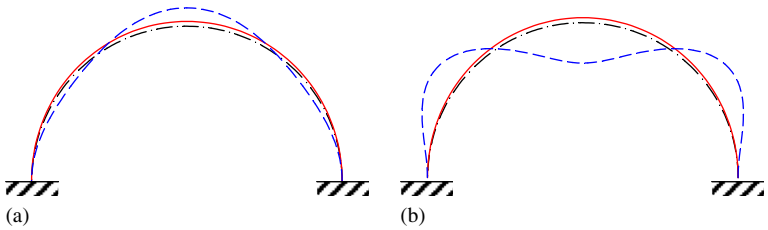

Fig. 4. Steady-state equilibrium configurations of a semi-circular pipe conveying fluid when: (a) $\overline{U} = 3.7$ and (b) $\overline{U} = 3.8$. Initial configuration (dash–dotted line); configuration for the nonlinear equilibrium equations (solid line); and configuration for the linearized equations (dashed line).

natural frequencies for the three models are listed and compared in Table 4; it was found that considerable differences exist in natural frequencies between the three models.

5. Conclusions

In this study, the steady-state equilibrium equations and linearized equations of motion were investigated for the dynamic analysis of a semi-circular fluid-conveying pipe. The validity of the linear and nonlinear

Table 4
Comparison of the three lowest dimensionless natural frequencies for the three models when the semi-circular pipe has a fluid velocity of $\overline{U} = 5$

	$\overline{\omega}_1$	$\overline{\omega}_2$	$\overline{\omega}_3$
Model I	2.8868	8.8887	16.0533
Model II	3.2457	9.2738	16.6548
Model III	3.1445	9.1910	16.2490
Difference between Models I and II	12.4%	4.3%	3.7%
Difference between Models I and III	8.9%	3.4%	1.2%

equilibrium equations was discussed, based on the equations of motion presented by Misra et al. [6]. The natural frequencies for the three models were computed and compared. This study found that the nonlinear steady-state equilibrium equations give more reasonable solutions than do the linear equilibrium equations. Furthermore, the equations proposed in this study were validated, and it was found that they provided more reliable natural frequencies than the equations of Ref. [6].

Acknowledgement

This work was supported by the research fund of Hanyang University (HY-2004-I).

References

[1] S.S. Chen, Vibration and stability of a uniformly curved tube conveying fluid, *Journal of Acoustical Society of America* 51 (1972) 223–232.
[2] S.S. Chen, Out-of-plane vibration and stability of curved tubes conveying fluid, *Journal of Applied Mechanics* 40 (1973) 362–368.
[3] J.L. Hill, C.G. Davis, The effect of initial forces on the hydrostatic vibration and stability of planar curved tube, *Journal of Applied Mechanics* 41 (1974) 355–359.
[4] R.W. Doll, C.D. Mote Jr., On the dynamic analysis of curved and twisted cylinders transporting fluids, *American Society of Mechanical Engineers Journal of Pressure Vessel Technology* 98 (1976) 143–150.
[5] A.K. Misra, M.P. Païdoussis, K.S. Van, On the dynamics of curved pipes transporting fluid. Part I: inextensible theory, *Journal of Fluids and Structures* 2 (1988) 221–244.
[6] A.K. Misra, M.P. Païdoussis, K.S. Van, On the dynamics of curved pipes transporting fluid. Part II: extensible theory, *Journal of Fluids and Structures* 2 (1988) 245–261.
[7] R.D. Blevins, *Formulas for Natural Frequency and Mode Shape*, Van Nostrand Reinhold, New York, 1979.